

Purchase  
Information

Information  
pour  
acheter

Titles  
Titres

←  
Article

→  
Article



**Geological Survey  
of Canada**

**CURRENT RESEARCH  
2001-E2**

***Spectral induced polarization measurements of sericite  
schist and ore samples from the Yellowknife mining  
district, Northwest Territories***

***N. Scromeda-Perez and T.J. Katsube***



Natural Resources  
Canada

Resources naturelles  
Canada

Canada

# CURRENT RESEARCH RECHERCHES EN COURS 2001

Purchase  
Information

Information  
pour  
acheter

Titles  
Titres

←  
Article

→  
Article



©Her Majesty the Queen in Right of Canada, 2001

Available in Canada from the  
Geological Survey of Canada Bookstore website at:  
<http://www.nrcan.gc.ca/gsc/bookstore> (Toll-free: 1-888-252-4301)

A copy of this publication is also available for reference by depository  
libraries across Canada through access to the Depository Services Program's  
website at <http://dsp-psd.pwgsc.gc.ca>

Price subject to change without notice

**All requests for permission to reproduce this work, in whole or in part, for purposes of commercial use, resale, or redistribution shall be addressed to: Earth Sciences Sector Information Division, Room 200, 601 Booth Street, Ottawa, Ontario K1A 0E8.**



## Spectral induced polarization measurements of sericite schist and ore samples from the Yellowknife mining district, Northwest Territories<sup>1</sup>

**N. Scromeda-Perez and T.J. Katsube**

*Mineral Resources Division, Ottawa*

*Scromeda-Perez, N. and Katsube, T.J., 2001: Spectral induced polarization measurements of sericite schist and ore samples from the Yellowknife mining district, Northwest Territories; Geological Survey of Canada, Current Research 2001-E2, 8 p.*

<sup>1</sup> Contribution to the 1999-2003 Canada-Northwest Territories Yellowknife Mining Camp Exploration Science and Technology (EXTECH-III) Initiative

### **Abstract**

*Spectral induced polarization measurements have been performed over a frequency range of 1–10<sup>6</sup> Hz on a suite of four mineralized and nonmineralized rock samples from the Giant mine and Con mine areas of the Yellowknife mining district, Northwest Territories. The purpose was to provide data for use in determining the electrochemical characteristics of the sulphides in these rocks.*

*Results indicate that the amplitude of complex resistivity ( $\rho^+$ ) and imaginary resistivity ( $\rho''$ ) in the  $\alpha$ -direction (perpendicular to foliation) consistently display larger values than those of the  $\beta$ - or  $\gamma$ -directions (parallel to foliation). The per cent frequency effect displays similar trends in the two directions ( $\alpha$ - and  $\beta$ - or  $\gamma$ -directions) with values in the range of 10–30% at the lower frequencies (<1000 Hz). This implies that the induced polarization effect of the sulphide minerals are being reflected in the data for all of these samples.*



## Résumé

*Quatre échantillons de roches minéralisées et non minéralisées provenant de la région des mines Giant et Con, dans le district minier de Yellowknife (Territoires du Nord-Ouest), ont été soumis à des mesures de polarisation provoquée spectrale dans une gamme de fréquences s'échelonnant de 1 Hz à 10<sup>6</sup> Hz. L'objectif de cette étude était d'obtenir des données permettant de déterminer les caractéristiques électrochimiques des sulfures présents dans ces roches.*

*Les résultats révèlent que l'amplitude de la résistivité complexe ( $\rho^+$ ) et de la résistivité imaginaire ( $\rho''$ ) dans la direction  $\alpha$  (perpendiculaire à la foliation), affiche, de façon constante, des valeurs plus élevées que celles obtenues dans les directions  $\beta$  ou  $\gamma$  (parallèles à la foliation). Le pourcentage de l'effet de fréquence montre des tendances semblables dans les deux directions (direction  $\alpha$  et direction  $\beta$  ou  $\gamma$ ) et des valeurs de l'ordre de 10 à 30% dans les basses fréquences ( $<1\ 000\text{Hz}$ ), ce qui signifie que l'effet de polarisation provoquée des sulfures se traduit dans les données, et ce, pour tous les échantillons étudiés.*

## INTRODUCTION

Electrical resistivity measurements have been performed on a suite of four mineralized and nonmineralized rock samples from the Giant mine and Con mine areas of the Yellowknife mining district, Northwest Territories. The purpose was to provide basic data for use in determining the spectral induced polarization (spectral IP) characteristics of these rocks. The samples include rocks from three sericite schist formations that run parallel to a gold-bearing vein, and one ore sample. This paper describes the methods and processes used to obtain the spectral IP data and document the results, in as much detail as considered necessary, for use in subsequent studies.



## METHOD OF INVESTIGATION

### *Sample preparation*

The four samples used in this study were selected from a set of thirty-four hand samples, collected underground by Jonathan Mwenifumbo and John Kerswill, from the Giant and Con mines, Yellowknife mining district, Northwest Territories. Three samples are from the Giant mine and one is from the Con mine. Information on sample location and lithology can be found elsewhere (Scromeda et al., 2000; Connell et al., 2000, 2001).

More than one specimen was usually cut from each sample into rectangular shapes with their edges either parallel or perpendicular to foliation. At least one specimen from each sample was used to determine the bulk electrical resistivity,  $\rho_r$ . In some cases, several rectangular specimens were cut from a single rock sample, in order to investigate the heterogeneities and anisotropy of the rock. The geometric characteristics of the specimens used for the 3-D  $\rho_r$  measurements are listed elsewhere (Scromeda et al., 2000). In this paper results are documented for only two of the three directions ( $\alpha$ - and  $\beta$ -directions or  $\alpha$ - and  $\gamma$ -directions) for each sample. The  $\alpha$ -direction is perpendicular to foliation and the  $\beta$ - and  $\gamma$ -directions are parallel to foliation (Connell et al., 2000, 2001).

### *Bulk electrical resistivity measurements*

The bulk electrical resistivity ( $\rho_r$ ) is determined from the complex electrical resistivity,  $\rho^*$ , method described in recent publications (e.g. Katsube and Salisbury, 1991). The complex electrical resistivity ( $\rho^*$ ) is measured over a frequency range of 1–10<sup>6</sup> Hz, with  $\rho_r$  representing a bulk electrical resistivity at frequencies of about 10<sup>2</sup>–10<sup>3</sup> Hz. It is a function of the pore structure and pore-fluid resistivity, and is



understood to exclude effects such as pore surface, dielectric, or electrode polarization (Katsube, 1975; Katsube and Walsh, 1987). Further details of the analytical procedure are described in Katsube et al. (1996). Results of the  $\rho_r$  measurements for the samples presented in this paper can be found elsewhere (e.g. Scromeda et al., 2000).

### *Spectral induced polarization measurements*

Spectral induced polarization measurements imply a frequency spectrum of the complex resistivity ( $\rho^*$ ) and complex conductivity ( $\sigma^*$ ) components, such as amplitude of complex resistivity ( $\rho^+$ ), real resistivity ( $\rho'$ ), imaginary resistivity ( $\rho''$ ), amplitude of complex conductivity ( $\sigma^+$ ), real conductivity ( $\sigma'$ ), and imaginary conductivities ( $\sigma''$ ). The inter-relationship between these parameters are as follows (Katsube, 2001):

$$\rho^* = \rho' - j\rho'', \quad (1)$$

$$\rho^+ = \sqrt{(\rho')^2 + \rho''^2}, \quad (2)$$

$$\sigma^* = 1/\rho^* = \sigma' + j\sigma'', \quad (3)$$

$$\sigma^+ = \sqrt{(\sigma')^2 + \sigma''^2}, \quad (4)$$

where

$$j = \sqrt{-1}. \quad (5)$$



In equivalent circuit analyses, where series circuits are dominant, as is in this case (Katsube, 2001), the use of complex conductivity curves are preferable. Although  $\sigma^+$  is equal to  $1/\rho^+$ , the same relationship does not apply to the other parameters. For example,  $\sigma' \neq 1/\rho'$ , and  $\sigma'' \neq 1/\rho''$ . Therefore, it is necessary to document this data in the complex conductivity format as well as the complex resistivity format. Although the frequency spectrum of all these parameters are routinely measured, only data for the bulk electrical resistivity ( $\rho_r$ ) has been reported in the past (e.g. Scromeda et al., 2000). The  $\rho_r$  is determined from the  $\rho'$  versus  $\rho''$  relationship (Cole-Cole diagrams). The frequency (f) spectrum of  $\rho^+$ ,  $\rho''$ ,  $\sigma^+$ , and  $\sigma''$  appear to be very useful (T.J. Katsube, J. Mwenifumbo, J. Kerswill, S. Connell, and N. Scromeda-Perez, online, [http://www.nrcan.gc.ca/gsc/mrd/extech3/2000\\_geo\\_forum\\_e.html](http://www.nrcan.gc.ca/gsc/mrd/extech3/2000_geo_forum_e.html)) in the spectral IP analysis. Therefore, the data for these parameters are documented in this paper.

## EXPERIMENTAL RESULTS

Results of the measurements are represented by the amplitude of the complex resistivity ( $\rho^+$ ), real resistivity ( $\rho'$ ), and imaginary resistivity ( $\rho''$ ), listed in **Tables 1a** and **1b**. The spectral IP effect is represented by the per cent frequency effect (PFE) defined as

$$\text{PFE} = (\rho^+_{i-1} - \rho^+_{i+1}) \times 100 / \rho^+_{i-1} \quad (6)$$

where  $i$  and  $i+1$  represent the frequency and an adjacent frequency in hertz for 12 frequencies over 6 decades where

$$i = 1, 3, 10, 30, 10^2, 3 \times 10^2, 10^3, 3 \times 10^3 \dots \dots 10^6.$$





These results are displayed in **Figures 1b, 2c, 3c, 4c, and 5c**. An example of a complete set of complex resistivity curves ( $\rho^+$ ,  $\rho'$ ,  $\rho''$  and PFE) are shown in Figure 1 for sample MYG-9 $\beta$ . The diagrams for  $\rho^+$  and  $\rho''$  as a function of frequency,  $f$ , are displayed in **Figures 2a, 3a, 4a, and 5a**. **Figures 2b, 3b, 4b, and 5b** display the results of the amplitude of the complex conductivity ( $\sigma^+$ ) and imaginary conductivity ( $\sigma''$ ) as a function of  $f$  where  $\sigma''$  is derived from

$$\sigma'' = \rho''/(\rho^+)^2. \quad (7)$$

Future studies for electrochemical capacitance effects on the sulphide minerals will focus on  $\rho''$  and  $\sigma''$  because of their out-of-phase characteristics. The  $\rho'$  and  $\sigma'$  contribute little information to this effect. Further details of these equations can be found elsewhere (e.g. Katsube, 1975; Katsube and Walsh, 1987).

## DISCUSSION AND CONCLUSIONS

The amplitude of complex resistivity ( $\rho^+$ ) and imaginary resistivity ( $\rho''$ ) versus frequency ( $f$ ) curves displayed in **Figures 2–5** clearly show that both  $\rho^+$  and  $\rho''$  in the  $\alpha$ -direction, which is perpendicular to foliation, consistently display the larger values than those of the  $\beta$ - or  $\gamma$ -directions, which are parallel to foliation. This is expected from previous results of the  $\rho_r$  measurements (Connell et al., 2000, 2001) for these rocks. Similarly, the amplitude of complex conductivity ( $\sigma^+$ ) and imaginary conductivity ( $\sigma''$ ) versus frequency ( $f$ ) curves displayed in Figures 2–5 clearly show that both  $\sigma^+$  and  $\sigma''$  in the  $\alpha$ -direction consistently display the smaller values than those of the  $\beta$ - or  $\gamma$ -directions, as would be expected.





The decrease in  $\rho^+$  and increases in  $\rho''$ ,  $\sigma^+$ , and  $\sigma''$  seen at the higher frequency end in all five figures are a result of the dielectric constant effects (T.J. Katsube, J. Mwenifumbo, J. Kerswill, S. Connell, and N. Scromeda-Perez, online, [http://www.nrcan.gc.ca/gsc/mrd/extech3/2000\\_geo\\_forum\\_e.html](http://www.nrcan.gc.ca/gsc/mrd/extech3/2000_geo_forum_e.html); Katsube, 2001). The per cent frequency effect (PFE) curves display similar trends in the two directions ( $\alpha$ - and  $\beta$ - or  $\gamma$ -directions) for all samples (**Fig. 2c**, **3c**, **4c**, **5c**), except for sample MYG-9 (**Fig. 3**). For sample MYG-11A (**Fig. 4**), the PFE values for the  $\beta$ -directions are slightly smaller than those for the  $\alpha$ -direction at the lower frequencies (<1000 Hz). The PFE values at the lower frequencies for all samples are generally in the range of 0–30%. This implies that the induced polarization (IP) effect of the sulphide minerals are likely being reflected in the data for sample MYG-9 (Fig. 3: ore sample), and to a certain degree in sericite schist samples MYG-11A (Fig. 4) and MYG-13 (**Fig. 5**). The PFE increase with increased frequency, at the higher frequencies (>10 000 Hz) for most samples, is likely a result of the dielectric effect (T.J. Katsube, J. Mwenifumbo, J. Kerswill, S. Connell, and N. Scromeda-Perez, online, [http://www.nrcan.gc.ca/gsc/mrd/extech3/2000\\_geo\\_forum\\_e.html](http://www.nrcan.gc.ca/gsc/mrd/extech3/2000_geo_forum_e.html)). Further detailed analyses of this data are planned for future studies.

## ACKNOWLEDGMENTS

The authors are grateful for the critical review of this paper and for the useful suggestions by J. Mwenifumbo (GSC). The authors thank Shauna Connell (GSC) for her contribution to the analysis of the results of this paper.



## REFERENCES

**Connell, S., Katsube, T.J., Hunt, P., and Kerswill, J.**

2001: Electrical mechanism of mineralized rocks from Giant and Con mine areas, Northwest Territories; Geological Survey of Canada, Current Research 2001-C2, 10 p.

**Connell, S., Scromeda, N., Katsube, T.J., and Mwenifumbo, J.**

2000: Electrical resistivity characteristics of mineralized and nonmineralized rocks from Giant and Con mine areas, Yellowknife, Northwest Territories; Geological Survey of Canada, Current Research 2000-E9; 7 p. (online; <http://www.nrcan.gc.ca/gsc/bookstore>).

**Katsube, T.J.**

1975: The electrical polarization mechanism model for moist rocks; Report of Activities, Part C; Geological Survey of Canada, Paper 75-1C, p. 353–360.

2001: An analytical procedure for determining spectral induced polarization characteristics of anisotropic rocks, Yellowknife mining district, Northwest Territories; Geological Survey of Canada, Current Research 2001-E3.

**Katsube, T.J. and Salisbury, M.**

1991: Petrophysical characteristics of surface core samples from the Sudbury structure; *in* Current Research, Part E; Geological Survey of Canada, Paper 91-1E, p. 265–271.

**Katsube, T.J. and Walsh, J.B.**

1987: Effective aperture for fluid flow in microcracks; International Journal of Rock Mechanics and Mining Sciences and Geomechanics Abstracts, v. 24, p. 175–183.

**Katsube, T.J., Palacky, G.J., Sangster, D.F., Galley, A.G., and Scromeda, N.**

1996: Electrical properties of disseminated sulphide ore samples from Snow Lake; *in* EXTECH I: Multidisciplinary Approach to Massive Sulphide Research in Rusty Lake-Snow Lake Greenstone Belts, Manitoba, (ed.) G.F. Bonham-Carter, A.G. Galley, and G.E.M. Hall; Geological Survey of Canada, Bulletin 426, p. 319–329.

**Scromeda, N., Connell, S., and Katsube, T.J.**

2000: Petrophysical properties of mineralized and nonmineralized rocks from Giant and Con mine areas, Northwest Territories; Geological Survey of Canada, Current Research 2000-E8; 7 p. (online; <http://www.nrcan.gc.ca/gsc/bookstore>)

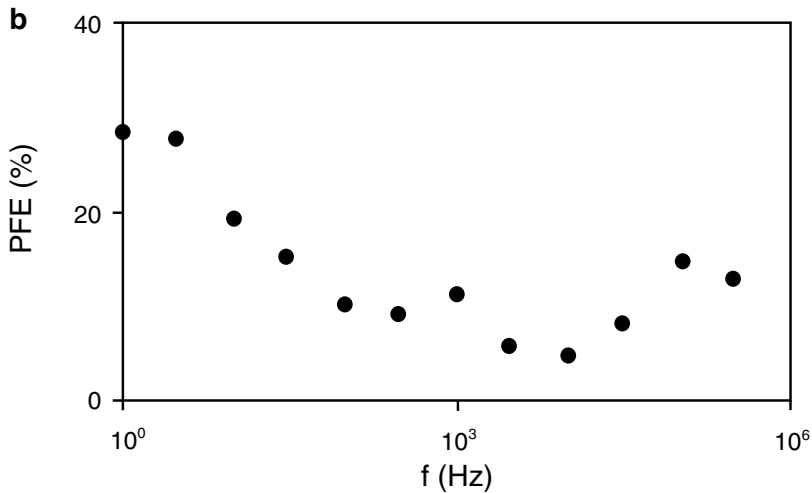
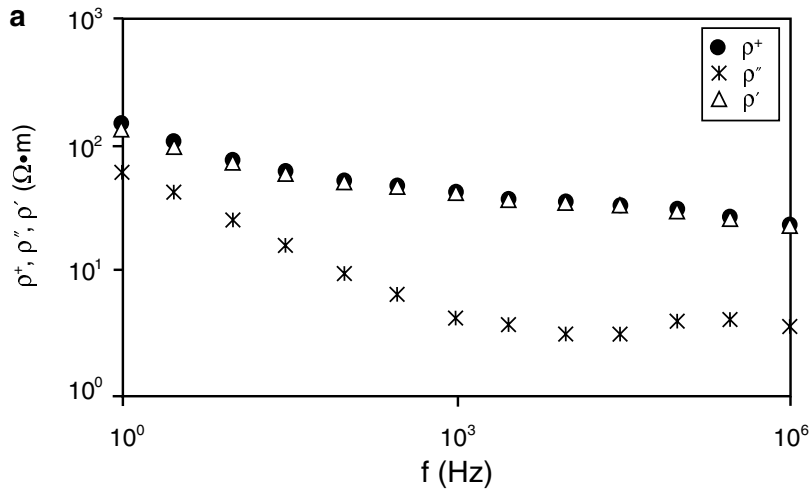


**Figure 1.** Typical examples of spectral IP curves for a low resistivity direction ( $\beta$ ) parallel to foliation for an ore sample/specimen, MYG-9: **a**) amplitude of complex resistivity ( $\rho^+$ ), real resistivity ( $\rho'$ ), and imaginary resistivity ( $\rho''$ ) as a function of frequency ( $f$ ), and **b**) per cent frequency effect (PFE) as a function of  $f$ .

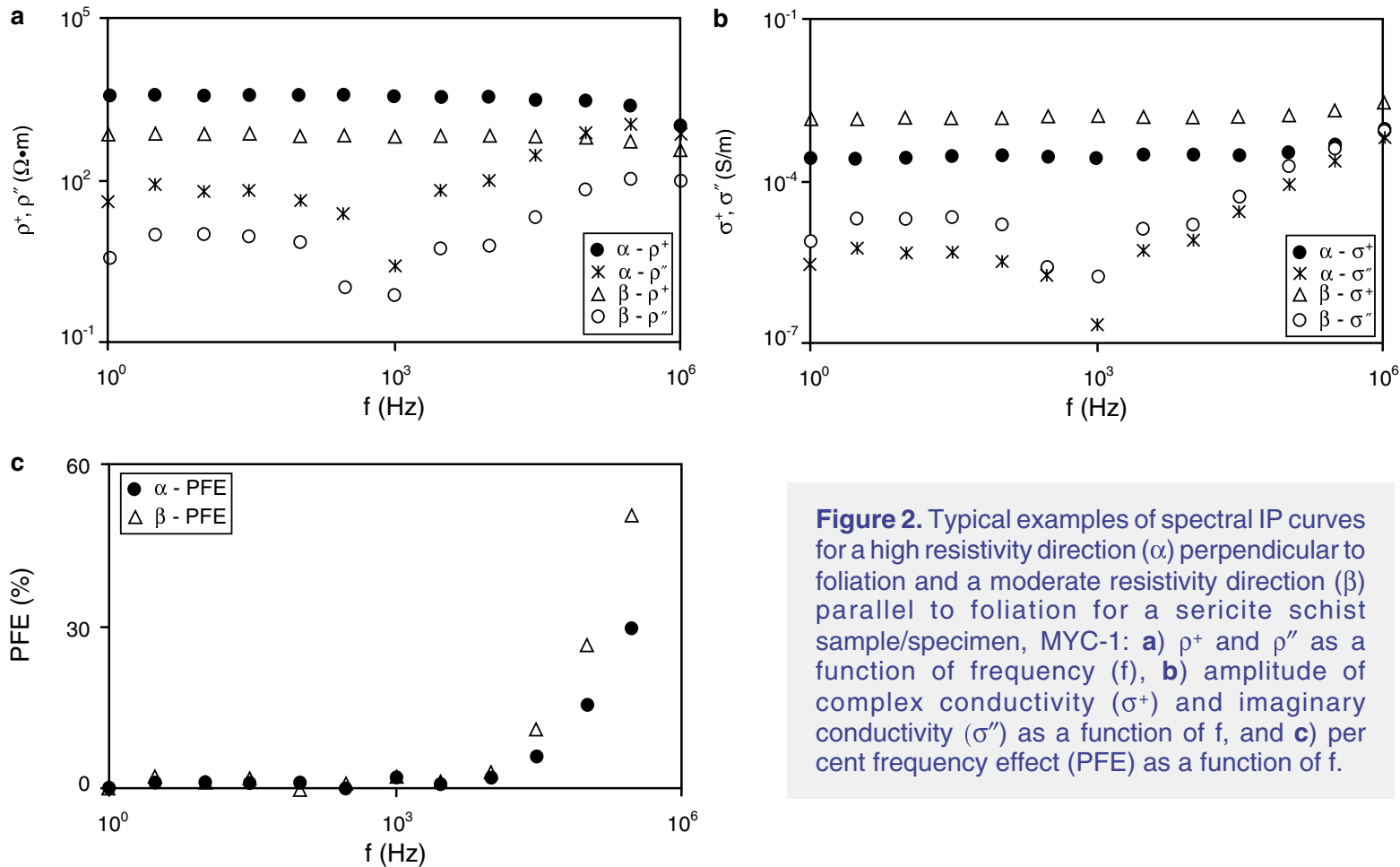


**Figure 2.** Typical examples of spectral IP curves for a high resistivity direction ( $\alpha$ ) perpendicular to foliation and a moderate resistivity direction ( $\beta$ ) parallel to foliation for a sericite schist sample/specimen, MYC-1: **a**)  $\rho^+$  and  $\rho''$  as a function of frequency ( $f$ ), **b**) amplitude of complex conductivity ( $\sigma^+$ ) and imaginary conductivity ( $\sigma''$ ) as a function of  $f$ , and **c**) per cent frequency effect (PFE) as a function of  $f$ .

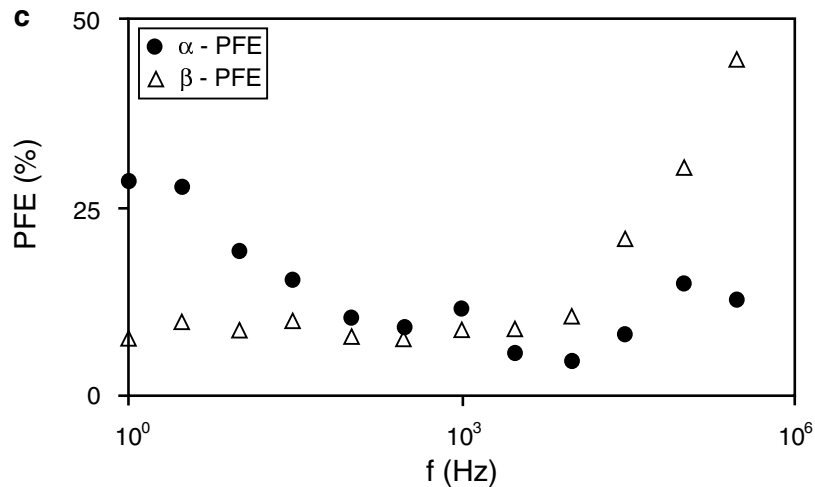
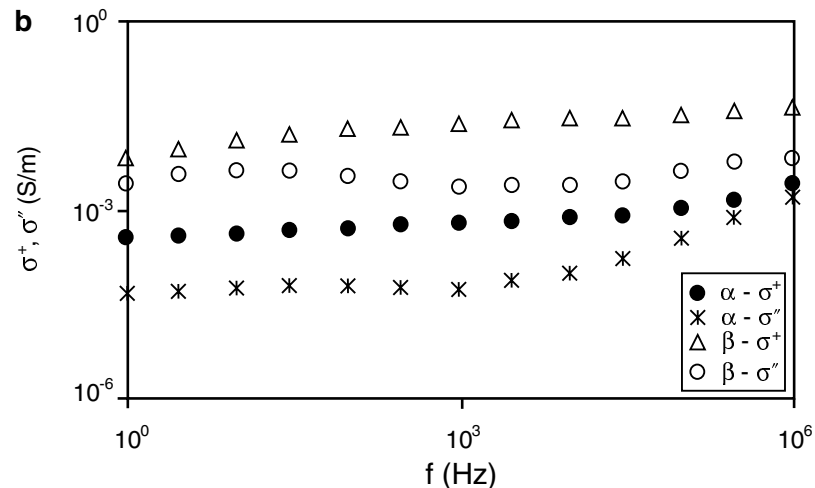
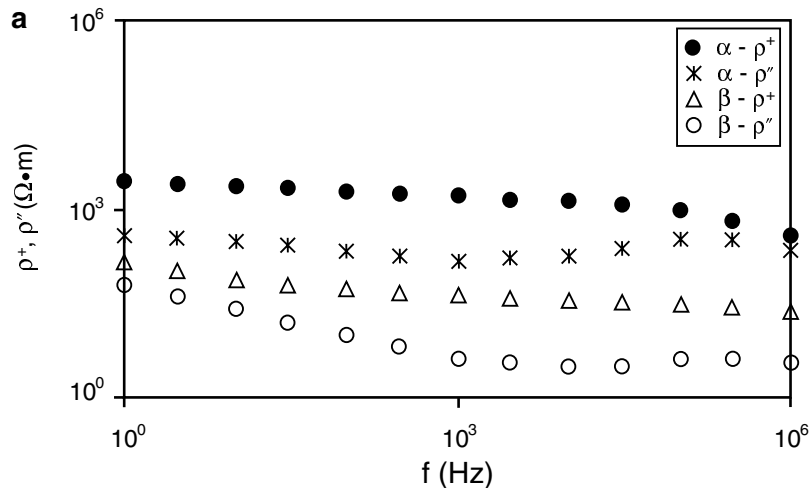


**Figure 3.** Typical examples of spectral IP curves for a high resistivity direction ( $\alpha$ ) perpendicular to foliation and a low resistivity direction ( $\beta$ ) parallel to foliation for an ore sample/specimen, MYG-9: **a**)  $\rho^+$  and  $\rho''$  as a function of frequency ( $f$ ), **b**)  $\sigma^+$  and  $\sigma''$  as a function of  $f$ , and **c**) per cent frequency effect (PFE) as a function of  $f$ .

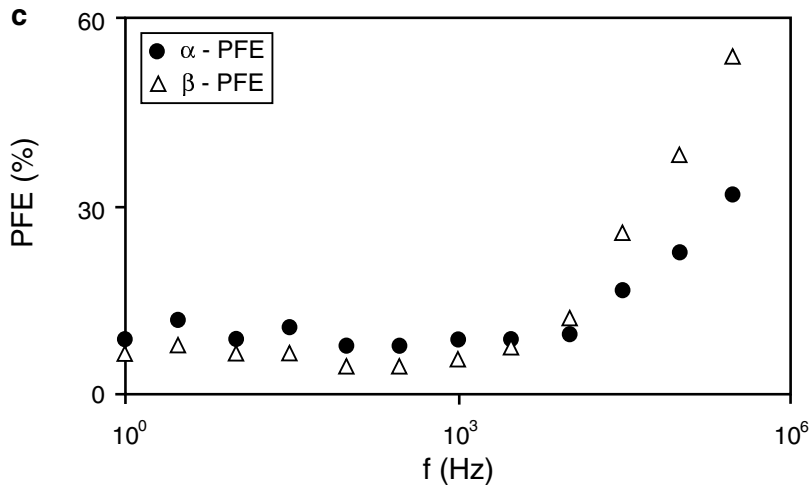
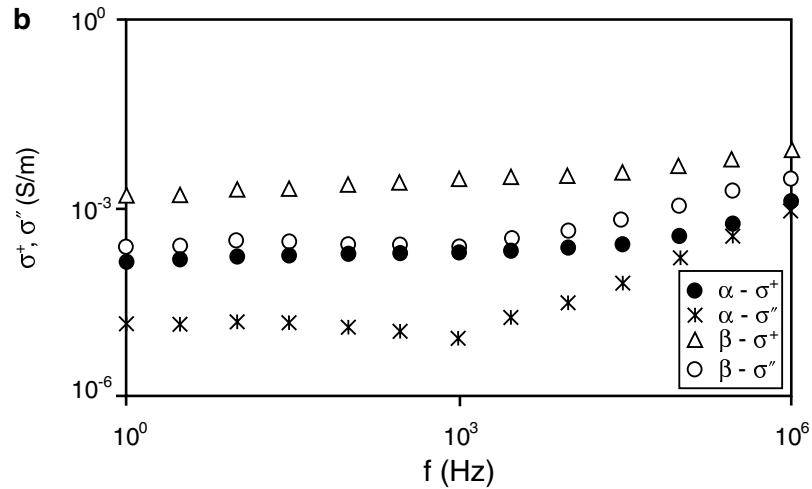
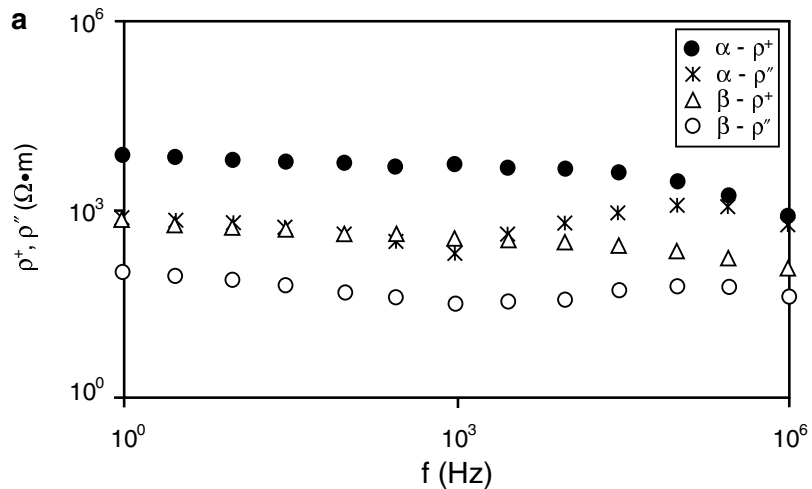


**Figure 4.** Typical examples of spectral IP curves for a high resistivity direction ( $\alpha$ ) perpendicular to foliation and a moderate resistivity direction ( $\beta$ ) parallel to foliation for a sericite schist sample/specimen, MYG-11a: **a**)  $\rho^+$  and  $\rho''$  as a function of frequency ( $f$ ), **b**)  $\sigma^+$  and  $\sigma''$  as a function of  $f$ , and **c**) per cent frequency effect (PFE) as a function of  $f$ .

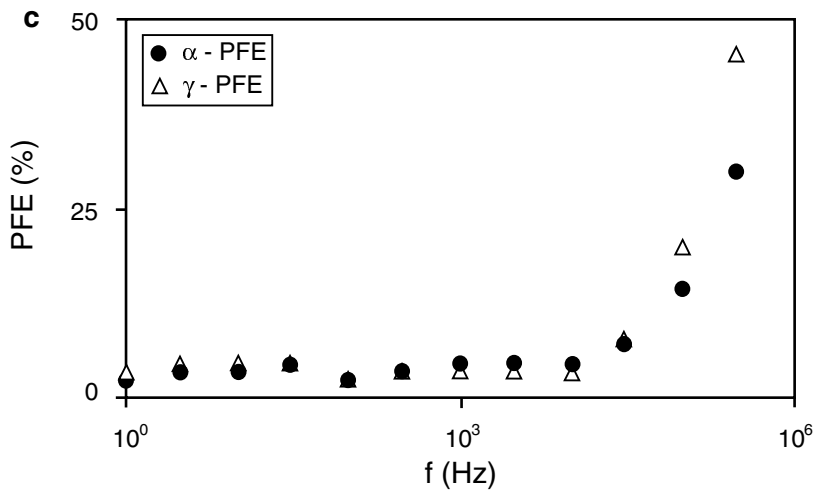
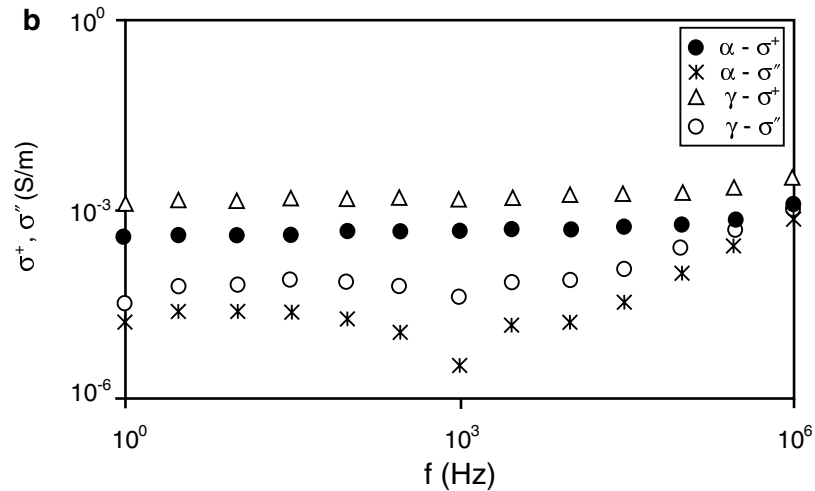
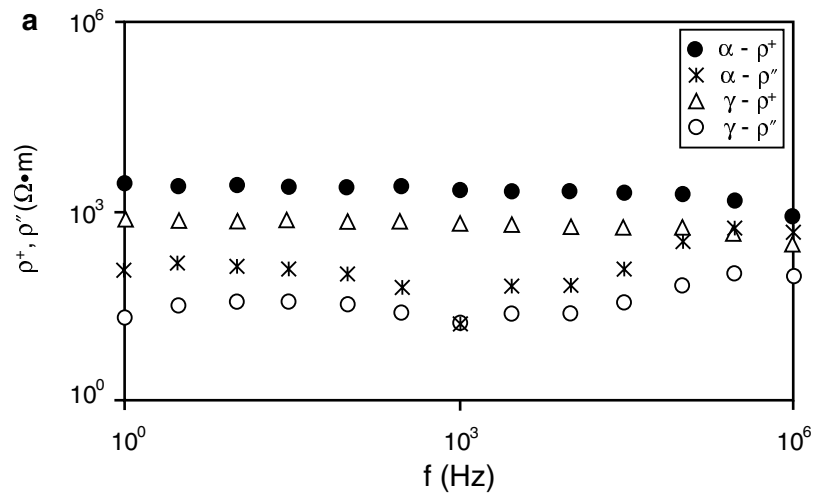


**Figure 5.** Typical examples of spectral IP curves for a high resistivity direction ( $\alpha$ ) perpendicular to foliation and a moderate resistivity direction ( $\gamma$ ) parallel to foliation for a sericite schist sample/specimen, MYG-13: **a**)  $\rho^+$  and  $\rho''$  as a function of frequency ( $f$ ), **b**)  $\sigma^+$  and  $\sigma''$  as a function of  $f$ , and **c**) per cent frequency effect (PFE) as a function of  $f$ .



**Table 1a.** Results for amplitude of complex ( $\rho^+$ ), real ( $\rho'$ ), and imaginary ( $\rho''$ ) electrical resistivity measurements for samples MYC-1 (sericite schist from the Con mine) and MYG-9 (ore from the Giant mine) over a frequency range of 1– $10^6$  Hz.

Frequency (Hz)	MYC-1 $\alpha$ ( $10^3 \Omega \cdot m$ )			MYC-1 $\beta$ ( $10^3 \Omega \cdot m$ )			MYG-9 $\alpha$ ( $10^3 \Omega \cdot m$ )			MYG-9 $\beta$ ( $10^3 \Omega \cdot m$ )		
	$\rho^+$	$\rho'$	$\rho''$	$\rho^+$	$\rho'$	$\rho''$	$\rho^+$	$\rho'$	$\rho''$	$\rho^+$	$\rho'$	$\rho''$
1	3.749	3.749	0.039	0.692	0.692	0.004	2.763	2.739	0.366	0.148	0.135	0.061
3	3.749	3.748	0.079	0.692	0.691	0.010	2.549	2.525	0.346	0.106	0.097	0.042
10	3.664	3.663	0.064	0.684	0.684	0.010	2.298	2.276	0.316	0.077	0.072	0.025
30	3.622	3.621	0.063	0.676	0.676	0.009	2.095	2.077	0.274	0.062	0.060	0.016
$10^2$	3.539	3.539	0.043	0.668	0.668	0.007	1.889	1.875	0.227	0.052	0.051	0.010
$3 \times 10^2$	3.539	3.539	0.024	0.660	0.660	0.001	1.742	1.733	0.185	0.047	0.047	0.006
$10^3$	3.499	3.499	0.003	0.660	0.660	0.0008	1.607	1.601	0.145	0.043	0.042	0.004
$3 \times 10^3$	3.419	3.419	0.062	0.645	0.645	0.006	1.466	1.457	0.163	0.038	0.038	0.004
$10^4$	3.381	3.380	0.098	0.638	0.638	0.006	1.338	1.325	0.183	0.036	0.035	0.003
$3 \times 10^4$	3.274	3.262	0.281	0.624	0.623	0.021	1.195	1.172	0.237	0.034	0.034	0.003
$10^5$	2.912	2.817	0.737	0.586	0.582	0.065	0.951	0.893	0.325	0.031	0.031	0.004
$3 \times 10^5$	2.139	1.866	1.046	0.496	0.485	0.104	0.664	0.577	0.330	0.026	0.026	0.004
$10^6$	1.061	0.782	0.718	0.349	0.335	0.097	0.369	0.298	0.219	0.023	0.023	0.004

$\rho^+$  = Amplitude of complex electrical resistivity after 24 hours saturation with deionized water  
 $\rho'$  = Real electrical resistivity after 24 hours saturation with deionized water  
 $\rho''$  = Imaginary electrical resistivity after 24 hours saturation with deionized water

**Table 1b.** Results for amplitude of complex ( $\rho^*$ ), real ( $\rho'$ ), and imaginary ( $\rho''$ ) electrical resistivity measurements for MYG-11a and MYG-13 (sericite schist samples from the Giant mine) over a frequency range of 1–10<sup>6</sup> Hz.

Frequency (Hz)	MYG-11a $\alpha$ (10 <sup>3</sup> $\Omega\cdot\text{m}$ )			MYG-11a $\beta$ (10 <sup>3</sup> $\Omega\cdot\text{m}$ )			MYG-13 $\alpha$ (10 <sup>3</sup> $\Omega\cdot\text{m}$ )			MYG-13 $\gamma$ (10 <sup>3</sup> $\Omega\cdot\text{m}$ )		
	$\rho^*$	$\rho'$	$\rho''$	$\rho^*$	$\rho'$	$\rho''$	$\rho^*$	$\rho'$	$\rho''$	$\rho^*$	$\rho'$	$\rho''$
1	7.301	7.262	0.751	0.649	0.641	0.102	2.693	2.691	0.113	0.754	0.754	0.018
3	6.813	6.782	0.653	0.592	0.585	0.091	2.601	2.598	0.141	0.737	0.736	0.030
10	6.285	6.258	0.592	0.521	0.516	0.075	2.484	2.481	0.134	0.712	0.711	0.035
30	5.866	5.844	0.501	0.475	0.471	0.064	2.372	2.369	0.120	0.688	0.687	0.035
10 <sup>2</sup>	5.474	5.460	0.391	0.423	0.420	0.050	2.266	2.264	0.095	0.657	0.656	0.031
3x10 <sup>2</sup>	5.228	5.219	0.298	0.390	0.388	0.040	2.214	2.213	0.057	0.642	0.641	0.025
10 <sup>3</sup>	4.992	4.988	0.200	0.360	0.359	0.032	2.139	2.139	0.016	0.620	0.620	0.016
3x10 <sup>3</sup>	4.715	4.697	0.404	0.328	0.327	0.034	2.066	2.065	0.060	0.592	0.592	0.024
10 <sup>4</sup>	4.357	4.316	0.602	0.299	0.297	0.038	1.997	1.996	0.064	0.565	0.565	0.022
3x10 <sup>4</sup>	3.826	3.711	0.931	0.270	0.266	0.047	1.934	1.930	0.119	0.540	0.539	0.032
10 <sup>5</sup>	2.840	2.553	1.246	0.225	0.218	0.058	1.784	1.758	0.305	0.502	0.498	0.063
3x10 <sup>5</sup>	1.756	1.364	1.106	0.174	0.164	0.057	1.430	1.327	0.534	0.430	0.419	0.097
10 <sup>6</sup>	0.812	0.564	0.584	0.118	0.111	0.041	0.784	0.642	0.449	0.302	0.286	0.098

$\rho^*$  = Amplitude of complex electrical resistivity after 24 hours saturation with deionized water  
 $\rho'$  = Real electrical resistivity after 24 hours saturation with deionized water  
 $\rho''$  = Imaginary electrical resistivity after 24 hours saturation with deionized water